Reactions of New Organoplatinum(II) and -(IV) Complexes of 1,4-Diaza-1,3-butadienes with Light and Electrons. Emission vs Photochemistry and the Electronic Structures of Ground, Reduced, Oxidized, and Low-Lying Charge-Transfer Excited States†

Wolfgang Kaim,* Axel Klein, and Steffen Hasenzahl

Institut für Anorganische Chemie, Universität Stuttgart, Pfaffenwaldring 55, D-70550 Stuttgart, Germany

Hermann Stoll

Institut für Theoretische Chemie, Universität Stuttgart, Pfaffenwaldring 55, D-70550 Stuttgart, Germany

Stanislav Záliš and Jan Fiedler

J. Heyrovsky Institute of Physical Chemistry and Electrochemistry, Academy of Sciences of the Czech Republic, Dolejškova 3, CZ-18223 Prague, Czech Republic

Received August 18, 1997⊗

Complexes between the 1,4-disubstituted 1,4-diaza-1,3-butadiene chelate ligands RN═CHCH═NR (R-DAB; R = alkyl, aryl) and the organoplatinum fragments $PtMe_2$, $PtMe_4$, and $PtMes_2$ (Mes = mesityl) were prepared and characterized with respect to their electronic structures. All compounds are distinguished by low-energy charge-transfer transitions to low-lying π^* orbitals of the R-DAB ligands, either from metal d orbitals (Pt^{II}) or from metal−carbon σ bond combinations (Pt^{IV}). These spectral assignments are supported by DFT calculations on model complexes between HN═CHCH═NH and $PtMe_2$ or $PtMe_4$. The calculations also reproduce the structural results for the complex between CyN═CHCH═NCy and $PtMe_4$, which exhibits significantly longer Pt−C bonds to the axial methyl groups. The distinct solvatochromism of the long-wavelength transitions is described, as are the UV/vis spectroelectrochemical results for reversible reduction to Pt^{IV}(R-DAB$^{\bullet-}$) or Pt^{II}(R-DAB$^{\bullet-}$) species (no evidence for a Pt^{I} state). In contrast, the oxidation is electrochemically irreversible except for the dimesitylplatinum compounds. The electrochemical potentials of corresponding $PtMe_2$ and $PtMe_4$ compounds are very similar, demonstrating that the binding of two additional methyl carbanions compensates for the effect of the higher metal oxidation state. While the organoplatinum(II) species are emissive, the tetramethylplatinum(IV) complexes are photoreactive and undergo metal-to-ligand methyl transfer reactions—in agreement with the structurally confirmed weaker bonding to the axial methyl groups.

Introduction

Platinum(II) and -(IV) complexes with nitrogen-donor-containing ligands have found interest as chemotherapeutic agents (cytostatica),[1] as catalysts,[2] and as photoemissive[3] or redox-active species.[4] The latter often involve π-accepting chelate ligands of the α-diimine type such as aromatic 2,2′-bipyridine[3i,4c,f] or 1,10-phenanthrolines.[4g] Detailed photophysical studies,[3] calculations,[3d,4j,k] structure determinations,[3c,d,4c,e] and (spectro)electrochemical and EPR studies of generated paramagnetic species[4] have been used recently to elucidate the nature of these systems (L)PtX_n in ground, reduced, oxidized, or low-lying excited states. The last may include ligand-field (LF) and metal-to-ligand charge-transfer (MLCT) excited states,[3] with particular emphasis on possible intermolecular interactions in square planar systems (α-diimine)PtX_2.[3f,i,o]

Considering the electronic complexity of these compounds,[3,4] the use of organic substituents as coligands X seems attractive due to the variability of such groups. For instance, the use of axially protecting mesityl (Mes, 2,4,6-trimethylphenyl) substituents in $PtMes_2$(α-diimine) compounds has allowed us to slow down the undesired addition of nucleophiles to the one-electron-oxidized monomeric platinum(III) states [$PtMes_2$(α-

† Dedicated to Professor Manfred Weidenbruch on the occasion of his 60th birthday.

⊗ Abstract published in *Advance ACS Abstracts,* December 15, 1997.

(1) (a) Farrell, N. in *Transition Metal Complexes as Drugs and Chemotherapeutic Agents*; James, B. R., Ugo, R., Eds.; Reidel-Kluwer: Dordrecht, The Netherlands, 1989; p 46. (b) Bloemink, M. J.; Reedijk, J. In *Metal Ions in Biological Systems*; Sigel, H., Sigel, A., Eds.; Marcel Dekker: New York, 1996; Vol. 32, p 641. (c) Sundquist, W. I.; Lippard, S. J. *Coord. Chem. Rev.* **1990**, *100,* 293.

(2) Stahl, S. S.; Labinger, J. A.; Bercaw, J. E. *J. Am. Chem. Soc.* **1996**, *118,* 5961.

S0276-7333(97)00736-X CCC: $15.00
Publication on Web 01/01/1998

diimine)]$^{+}$.[4c,f] It was thus possible to obtain spectroelectrochemical data on monomeric organometallic Pt(III) systems[4f] and to use the corresponding Pt(II)/Pt(III) half-wave potentials in correlations between optical data (absorption or emission energies) and electrochemical results.[4f]

Employing the smaller and simpler 1,4-diaza-1,3-butadienes R-DAB[5−7] as chelate ligands instead of aromatic systems such as 2,2′-bipyridine, we hoped to further simplify the spectroscopy (UV/vis, IR, EPR) of the complexes.[4e] Smaller systems may not only provide clearer experimental informations (i.e. diminished spectral overlap), but also should allow us to obtain a reliable basis for quantum-chemical calculations. Furthermore, the variation of N-substituents R from electron-releasing alkyl to electron-accepting aryl groups, including axially shielding 2,6-dimethylphenyl substituents,[7] should provide clues as to the electronic and/or steric effects governing various physical properties.

We now wish to present results for organoplatinum complexes which contain R-DAB as a chelating "noninnocent" ligand. Complexes of R-DAB have been widely used in fundamental coordination chemistry[5−7] and catalysis;[8] they are often considered "better"[6] π acceptors than 2,2′-bipyridine due to their lower lying π^* acceptor level and their larger LUMO coefficients at the coordinating nitrogen centers.

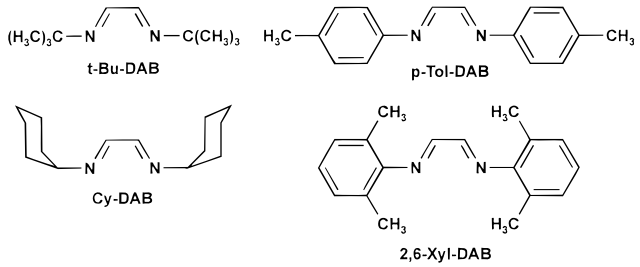

The spectroscopy and structures of a set of CyN═CHCH═NCy complexes with $PtMe_2$ and $PtMe_4$ fragments have been recently reported.[4e] In this work we present results for the following compounds (Cy = 1-cyclohexyl, *p*-Tol = 4-tolyl, 2,6-Xyl = 2,6-dimethylphenyl):

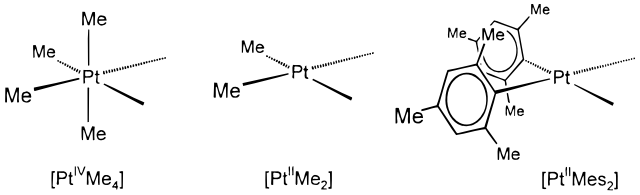

$PtMe_2$(R-DAB): R = *t*-Bu, Cy, *p*-Tol, 2,6-Xyl

$PtMe_4$(R-DAB): R = *t*-Bu, Cy, *p*-Tol, 2,6-Xyl

$PtMes_2$(R-DAB): R = Cy, *p*-Tol

$PtMe_4$(*t*-Bu-Pyca): *t*-Bu-Pyca = pyridine-2-carbaldehyde *tert*-butylimine

$PtMe_n$(TMEDA): n = 2,4

The methyl group (Me) as the most simple organic substituent and the mesityl function as axially protecting aryl group were used as organic coligands. As methods to elucidate the nature of ground, reduced, oxidized, and charge-transfer excited states we used optical absorption spectroscopy, including studies of the solvatochromic behavior, emission spectroscopy at ambient temperatures, and cyclic voltammetry in combination with spectroscopy (spectroelectrochemistry). Details of EPR measurements on paramagnetic states have been published elsewhere.[4n]

As compounds related to the PtR_n(R-DAB) species we also studied $PtMe_4$(*t*-Bu-Pyca) with pyridine-2-carbaldehyde *tert*-butylimine as mixed aromatic/nonaromatic α-diimine ligand;[9] for comparison we also synthesized the compounds $PtMe_n$(TMEDA) (n = 2,4) with the saturated chelate ligand 1,1,4,4-tetramethylethylenediamine (TMEDA).

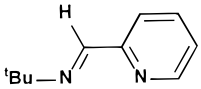

Experimental Section

Instrumentation. ^{1}H- and ^{13}C-NMR spectra were recorded on a Bruker AC 250 spectrometer. UV/vis/near-IR absorption

(3) (a) Miskowski, V. M.; Houlding, V. H. *Inorg. Chem.* **1989**, *28*, 1529. (b) Che, C.-M.; He, L.-Y.; Poon, C.-K.; Mak, C. W. *Inorg. Chem.* **1989**, *28*, 3081. (c) Biedermann, J.; Gliemann, G.; Klement, U.; Range; K.-J.; Zabel, M. *Inorg. Chem.* **1990**, *29*, 1884. (d) Biedermann, J.; Gliemann, G.; Klement, U.; Range, K.-J.; Zabel, M. *Inorg. Chim. Acta* **1990**, *169*, 63. (e) Kunkely, H.; Vogler, A. *J. Am. Chem. Soc.* **1990**, *112*, 5625. (f) Miskowski, V. M.; Houlding, V. H. *Inorg. Chem.* **1991**, *30*, 4446. (g) Chassot, L.; von Zelewsky, A. *Helv. Chim. Acta* **1986**, *69*, 1855. (h) Miskowski, V. M.; Houlding, V. H.; Che, C. M.; Wang, Y. *Inorg. Chem.* **1993**, *32*, 2518. (i) Houlding, V. H.; Miskowski, V. M. *Coord. Chem. Rev.* **1991**, *111*, 145. (j) Cornioley-Deuschel, C.; von Zelewsky, A. *Inorg. Chem.* **1987,** *26*, 3354. (k) von Zelewsky, A.; Belser, P.; Hayoz, P.; Dux, R.; Husa, X.; Suckling, A.; Stoeckli-Evans, H. *Coord. Chem. Rev.* **1994**, *132*, 75. (l) Chan, C.-W.; Cheng, L.-K.; Che, C.-M. *Coord. Chem. Rev.* **1994**, *132*, 87. (m) Cummings, S. D.; Eisenberg, R. *J. Am. Chem. Soc.* **1996**, *118*, 1949. (n) Peyratout, C. S.; Aldridge, T. K.; Crites, D. K.; McMillin, D. R. *Inorg. Chem.* **1995**, *34*, 4484. (o) Connick, W. B.; Henling, L. M.; Marsh, R. E.; Gray, H. B. *Inorg. Chem.* **1996**, *35*, 6261. (p) Donges, D.; Nagle, J. K.; Yersin, H. *Inorg. Chem.* **1997**, *36*, 3040.

(4) (a) Braterman, P. S.; Song, J.-I.; Vogler, C.; Kaim, W. *Inorg. Chem.* **1992**, *31*, 222. (b) Vogler, C.; Schwederski, B.; Klein, A.; Kaim, W. *J. Organomet. Chem.* **1992**, *436*, 367. (c) Klein, A.; Hausen, H.-D.; Kaim, W. *J. Organomet. Chem.* **1992**, *440*, 207. (d) Braterman, P. S.; Song, J.-I.; Wimmer, F. M.; Wimmer, S.; Kaim, W.; Klein, A.; Peacock, R. D. *Inorg. Chem.* **1992**, *31*, 5084. (e) Hasenzahl, S.; Hausen, H.-D.; Kaim, W. *Chem. Eur. J.* **1995**, *1*, 95. (f) Kaim, W.; Klein, A. *Organometallics* **1995**, *14*, 1176. (g) Klein, A.; Kaim, W.; Waldhör, E.; Hausen, H.-D. *J. Chem. Soc., Perkin Trans. 2* **1995**, 2121. (h) Klinger, R. J.; Huffman, R. J.; Kochi, J. K. *J. Am. Chem. Soc.* **1982**, *104*, 2147. (i) MacGregor, S. A.; McInnes, E.; Sorbie, R. J.; Yellowlees, L. J. in *Molecular Electrochemistry of Inorganic, Bioinorganic and Organometallic Compounds*; Pombeiro, A. J. L., McCleverty, J. A., Eds.; Kluwer Academic Publishers: Dordrecht, The Netherlands, 1993; p 503. (j) Collison, D.; Mabbs, F. E.; McInnes, E. J. L.; Taylor, K. J.; Welch, A. J.; Yellowlees, L. J. *J. Chem. Soc., Dalton Trans.* **1996**, 329. (k) Hill, M. G.; Bailey, J. A.; Miskowski, V. M.; Gray, H. B. *Inorg. Chem.* **1996**, *35*, 4585. (l) McInnes, E. J. L.; Welch, A. J.; Yellowlees, L. J. *J. Chem. Soc., Chem. Commun.* **1996**, 2393. (m) Klein, A.; Kaim, W.; Hornung, F. M.; Fiedler, J.; Zalis, S. *Inorg. Chim. Acta* **1997**, *264*, 269. (n) Klein, A.; Hasenzahl, S.; Kaim, W. *J. Chem. Soc., Perkin Trans. 2*, in press.

(5) van Koten, G.; Vrieze, K. *Adv. Organomet. Chem.* **1982**, *21*, 151.

(6) tom Dieck, H.; Franz, K.-D.; Hohmann, F. *Chem. Ber.* **1975**, *108*, 163.

(7) (a) Reinhardt, R.; Kaim, W., *Z. Anorg. Allg. Chem.* **1993**, *619*, 1998. (b) Greulich, S.; Kaim, W.; Stange, A.; Stoll, H.; Fiedler, J.; Zalis, S. *Inorg. Chem.* **1996**, *35*, 3998.

(8) Killian, C. M.; Johnson, L. K.; Brookhart, M. *Organometallics* **1997**, *16*, 2005.

spectra were recorded on a Bruins Instruments Omega 10 instrument. A Perkin-Elmer LS-3B fluorescence spectrometer served to record emission spectra. Cyclic voltammetry and differential pulse voltammetry were carried out using a three-electrode configuration (glassy-carbon working electrode, platinum counter electrode, Ag/AgCl reference) and a PAR 273 potentiostat and function generator with PAR M270/250 software. As internal standard the ferrocene/ferrocenium couple ($FeCp_2^{+/0}$) was used. The photochemical experiments were effected by irradiation of cooled dilute solutions (see text) with an HBO 50W/AC mercury vapor lamp or a 100 W halogen lamp. The wavelength range was adjusted using cutoff filters. Product analysis by GC was performed with Perkin-Elmer 8410 and Carlo Erba Fractovap 2150 instruments (column PS 086). GC−MS measurements were performed with a Finnigan 4500 quadrupole mass spectrometer. For spectroelectrochemical measurements we employed an optically transparent thin-layer electrolytic (OTTLE) cell.[10]

Materials. The R-DAB ligands[11] and the platinum precursor complexes $[Pt_2Me_8(\mu\text{-}SMe_2)_2]$,[12] $[Pt_2Me_4(\mu\text{-}SMe_2)_2]$,[13] and $(DMSO)_2PtMes_2$[14] were obtained following literature procedures. $PtMe_2$(TMEDA) was obtained according to published procedures.[15] Other reagents were used as commercially available. All preparations and physical measurements were carried out in dried solvents under an argon atmosphere, using Schlenk techniques. Furthermore, the tetramethylplatinum(IV) compounds had to be prepared and studied in the absence of intense light. Solvents for photochemical experiments were additionally degassed by three subsequent freeze−pump−thaw cycles.

General Procedure for Tetramethylplatinum Complexes $PtMe_4$(R-DAB). In a typical reaction, 0.4 mmol of the R-DAB ligand was added to a solution of 0.127 g (0.2 mmol) of $[Pt_2Me_8(\mu\text{-}SMe_2)_2]$ in 20 mL of diethyl ether. Within a few minutes the solutions become intensely colored. After stirring at ambient temperatures overnight in the absence of light the volume of the solution was reduced to 10 mL. At −30 °C microcrystalline solids precipitated from this solution (red for for the complex with *t*-Bu-DAB, brown for those with *p*-Tol- and 2,6-Xyl-DAB, and purple for $PtMe_4$(Cy-DAB)). They were collected on a microporous frit, washed with hexane, and dried *in vacuo*. Yield for $PtMe_4$(*t*-Bu-DAB): 115 mg (0.27 mmol, 68%). Anal. Calcd for $C_{14}H_{32}N_2Pt$: C, 39.70; H, 7.62; N, 6.62. Found: C, 39.32; H, 7.75; N, 6.32. $PtMe_4$(Cy-DAB): yield 90 mg (0.19 mmol, 47%). Anal. Calcd for $C_{18}H_{36}N_2Pt$: C, 45.46; H, 7.63; N, 5.89. Found: C, 245.81; H, 7.75; N, 5.76. $PtMe_4$(*p*-Tol-DAB): yield 135 mg (0.276 mmol, 69%). Anal. Calcd for $C_{20}H_{28}N_2Pt$: C, 48.87; H, 5.74; N, 5.70. Found: C, 48.41; H, 5.67; N, 5.69. $PtMe_4$(2,6-Xyl-DAB): yield 88 mg (0.17 mmol, 29%). Anal. Calcd for $C_{22}H_{32}N_2Pt$: C, 50.85; H, 6.21; N, 5.39. Found: C, 50.76; H, 6.09; N, 5.14.

$PtMe_4$(*t*-Bu-Pyca). The synthesis proceeded in the same way as for the R-DAB complexes. Yield: 100 mg of an orange solid (0.24 mmol, 60%). Anal. Calcd for $C_{14}H_{26}N_2Pt$: C, 40.28; H, 6.28; N, 6.71. Found: C, 39.85; H, 6.18; N, 6.45.

$PtMe_4$(TMEDA). A solution of 127 mg (0.2 mmol) of $Pt_2Me_8(\mu\text{-}SMe_2)_2$ and 46 mg (0.4 mmol) of *N*,*N*,*N*′,*N*′-tetramethylethylenediamine in 20 mL of diethyl ether was stirred at ambient temperature for 10 h. The reaction mixture was concentrated to 5 mL, and 10 mL of *n*-hexane was added. The mixture was kept at −30 °C to accomplish precipitation of the colorless product. Yield: 105 mg (0.28 mmol, 71%). Anal. Calcd for $C_{10}H_{28}N_2Pt$: C, 32.34; H, 7.60; N, 7.54. Found: C, 31.67; H, 7.10; N, 7.44.

General Procedure for Dimethylplatinum Complexes $PtMe_2$(R-DAB). In typical reactions, 0.4 mmol of the R-DAB ligand was added to a solution of 0.115 g (0.2 mmol) of $[Pt_2Me_4(\mu\text{-}SMe_2)_2]$ in a mixture of 15 mL of benzene and 10 mL of diethyl ether. The solution was stirred overnight at ambient temperature. After removal of the solvents the resulting solids were dissolved in a sufficient amount of diethyl ether. At −30 °C microcrystalline solids precipitated from this solution (dark green for the complex with *p*-Tol-DAB, greenish blue for that with 2,6-Xyl-DAB, and dark purple for the compound with Cy-DAB). They were collected on a microporous glass frit, washed with 10 mL of hexane, and dried *in vacuo*. Yield for $PtMe_2$(Cy-DAB): 71.3 mg (0.16 mmol, 40%). Anal. Calcd for $C_{16}H_{30}N_2Pt$: C, 43.13; H, 6.79; N, 6.29. Found: C, 43.29; H, 6.60; N, 6.02. Yield for $PtMe_2$(*p*-Tol-DAB): 120 mg (0.26 mmol, 65%). Anal. Calcd for $C_{18}H_{22}N_2Pt$: C, 46.85; H, 4.81; N, 6.07. Found: C, 46.66; H, 4.69; N, 6.06. Yield for $PtMe_2$(2,6-Xyl-DAB): 49 mg (0.1 mmol, 25%). Anal. Calcd for $C_{20}H_{26}N_2Pt$: C, 49.07; H, 5.35; N, 5.72. Found: C, 48.94; H, 5.51; N, 5.35. With *t*-Bu-DAB the corresponding complex could be detected by ^1H NMR but could not be isolated.

General Procedure for Dimesitylplatinum Complexes $PtMes_2$(R-DAB). In typical reactions, 150 mg (0.225 mmol) of bis(dimethyl sulfoxide)dimesitylplatinum(II) was suspended together with 0.26 mmol of the corresponding R-DAB ligand in 40 mL of toluene and heated under reflux for 20 h. The reaction is complete when the IR-active $\nu_{S=O}$ vibration of the precursor complex has vanished.[16] The reaction mixture is then left at 4 °C overnight, and the resulting dark microcrystalline precipitate is filtered, washed with diethyl ether, and dried *in vacuo*. Yield for $PtMes_2$(Cy-DAB): 92.7 mg (0.142 mmol, 63%) of a purple solid. Anal. Calcd for $C_{32}H_{46}N_2Pt$: C, 58.79; H, 7.09; N, 4.29. Found: C, 58.97; H, 7.05; N, 4.07. Yield for $PtMes_2$(*p*-Tol-DAB): 78.4 mg (0.117 mmol, 53%) of a dark green solid. Anal. Calcd for $C_{34}H_{38}N_2Pt$: C, 60.97; H, 5.72; N, 4.18. Found: C, 61.79; H, 5.48, N, 4.05.

Photolysis of $PtMe_4$(*t*-Bu-DAB). In preliminary experiments acetone, THF, diethyl ether, toluene, benzene, and pyridine were tested as solvents for the photolysis of $PtMe_4$(*t*-Bu-DAB). A mixture of products resulted in each case, and acetone was eventually chosen as the solvent with the least complications.

A dilute solution containing 150 mg (0.36 mmol) of $PtMe_4$(*t*-Bu-DAB) in 60 mL of dried and deaerated acetone was irradiated in a water-cooled Schlenk vessel using a halogen lamp (λ > 475 nm; cut-off filter GG 475). Irradiation was stopped after about 15 min when the sample had turned completely colorless. (Left unattended, this solution decomposed, forming a brown solution and a precipitate of elemental platinum.) The colorless solution was evaporated to about 5 mL, and 10 mL of *n*-hexane was added. However, even after 2 days at −30 °C there was no formation of any solid. After complete removal of the solvent under reduced pressure, a yellowish viscous oil remained. The complex mixture of methylplatinum-containing substances could not be separated using either chromatographic methods or fractionated crystallization. ^1H-NMR ($CDCl_3$): δ −0.47(m), 0.05 (s), 0.19 (s), 0.14, 0.30, 0.20, 0.71 (s, $^2J(^{195}Pt^1H)$ = 71.2 Hz), 0.89, 0.90, 0.93, 0.97, 1.04, 1.06, 1.11, 1.16, 1.17, 1.20, 1.23, 1.26, 1.30, 1.33 (s), 1.44 (s), 2.13 (s), 2.28 (s), 2.61 (s), 3.45 (m), 3.56 (m), 3.98 (s), 3.99 (d, J(HH) = 5.1 Hz), 4.43 (s), 7.38 (d, J(HH) = 5.4 Hz), 7.43

(9) (a) Polm, L. H.; van Koten, G.; Elsevier, C. J.; Vrieze, K.; van Saften, B. F. K.; Stam, C. H. *J. Organomet. Chem.* **1986**, *304*, 353. (b) Stahl, T.; Kasack, V.; Kaim, W. *J. Chem. Soc., Perkin Trans. 2* **1995**, 2127.

(10) Krejcik, M.; Danek, M.; Hartl, F. *J. Electroanal. Chem. Interfacial Electrochem.* **1991**, *317*, 179.

(11) (a) tom Dieck, H.; Renk, I. W. *Chem. Ber.*, **1971**, *104*, 92. (b) tom Dieck, H.; Svoboda, M.; Greiser, T. *Z. Naturforsch.* **1981**, *36B*, 823.

(12) Scott, J. D.; Puddephatt, R. J. *Organometallics* **1983**, *2*, 1643.

(13) Scott, J. D.; Puddephatt, R. J. *Organometallics* **1986**, *5*, 1538.

(14) Eaborn, C.; Kundu, K.; Pidcock, A. *J. Chem. Soc., Dalton Trans.* **1981**, 933.

(15) (a) Yang, D.-S.; Bancroft, G. M.; Dignard-Bailey, L.; Puddephatt, R. J.; Tse, J. S. *Inorg. Chem.* **1990**, *29*, 2487. (b) Appleton, F. G.; Hall, J. R.; Neale, D. W.; Williams, M. A. *J. Organomet. Chem.* **1984**, *276*, C73.

(16) Cotton, F. A.; Francis, R.; Horrocks, W. D., Jr. *J. Phys. Chem.* **1969**, *64*, 1534.

Table 1. ^{1}H-NMR Data of Platinum Complexes and Free Ligands in $CDCl_3$ at 25 °C[a]

compd	$Pt^{ax}CH_3$[b]	$Pt^{eq}CH_3$[b]	N=CH[b]	R
t-Bu-DAB			7.90	1.22[c]
$PtMe_4$(*t*-Bu-DAB)	−0.38 (44.3)	1.08 (73.5)	8.60 (23.5)	1.46[c]
$PtMe_2$(*t*-Bu-DAB)		1.33 (86.4)	8.93 (26.5)	1.55[c]
Cy-DAB			7.90	3.09,[d] 1.09−1.74[e]
$PtMe_4$(Cy-DAB)	−0.54 (45.9)	0.75 (71.3)	8.54 (31.6)	4.10,[d] 1.13−2.06[e]
$PtMe_2$(Cy-DAB)		1.40 (84.9)	8.91 (35.0)	4.18,[d] 1.09−2.22[e]
p-Tol-DAB			8.40	2.37,[f] 7.21[b,g]
$PtMe_4$(*p*-Tol-DAB)	−0.24 (46.0)	0.72 (73.5)	8.63 (28.3)	2.40,[f] 7.07,[g,h] 7.25,[g,h]
$PtMe_2$(*p*-Tol-DAB)		1.78 (87.7)	9.30 (28.6)	2.40,[f] 7.28−7.34[g]
$PtMes_2$(*p*-Tol-DAB)			9.23 (28.3)	2.25,[f] 6.83,[g] 6.93,[g,i]
2,6-Xyl-DAB			8.11	2.17,[f] 6.86−7.10[g,j]
$PtMe_4$(2,6-Xyl-DAB)	−0.04 (46.0)	0.61 (72.8)	8.75 (29.6)	2.21,[f] 7.06−7.13[g,j]
$PtMe_2$(2,6-Xyl-DAB)		1.65 (87.4)	9.39 (34.8)	2.24,[f] 7.11−7.21[g]
t-Bu-Pyca			8.27	1.22,[c] 7.16,[k] 7.60,[l] 7.93,[m] 8.52[n]
$PtMe_4$(*t*-Bu-Pyca)	−0.52 (44.3)	0.95, 1.09 (73.5, 73.1)	8.67 (26.1)	1.51,[c] 7.44,[k] 7.82,[l] 7.88,[m] 8.84[n]
TMEDA			2.24[b,o]	2.10[b,p]
$PtMe_4$(TMEDA)	−0.32 (40.6)	0.58 (73.3)	2.60[b,o] (6.3)	2.45[b,p] (12.4)
$PtMe_2$(TMEDA)		0.39 (85.4)	2.61[b,o] (11.4)	2.65[b,p] (21.5)

[a] Chemical shifts d in ppm, $J(^{195}Pt^1H)$ coupling constants (in Hz) in parentheses. [b] Singlet. [c] $C(CH_3)_3$ (singlet). [d] $NCH(C_5H_{10})$ (multiplet). [e] $NCH(C_5H_{10})$ (multiplet). [f] CH_3(singlet). [g] *CH* (phenyl H). [h] Doublet, $^3J(^1H^1H) = 8.2$ Hz. [i] Further signals: 6.36 (s, 4H, Mes *H*, $J(^{195}Pt^1H) = 15.1$ Hz), 2.19 (s, 12H, Mes o-CH_3), 2.13 (s, 6H, Mes *p*-CH_3). [j] Multiplet. [k] Pyridyl-H*5* (dt). [l] Pyridyl-H*4* (t). [m] Pyridyl-H*3* (dd). [n] Pyridyl-H*6* (d). [o] N-CH_2-CH_2-N. [p] $N(CH_3)_2$.

(s), 7.61 (s). ^{13}C-NMR ($CDCl_3$): δ −15.8 ($J(^{195}Pt^{13}C) = 722.0$ Hz), −11.4 ($J(^{195}Pt^{13}C) = 745.8$ Hz), −11.2, −9.1, -4.9, −3.4, 1.0, 15.9, 21.6, 26.6 ($J(^{195}Pt^{13}C) = 7.3$ Hz), 27.4 - 32.2 (13 peaks), 51.1, 52.4, 53.8, 56.0, 61.8 ($J(^{195}Pt^{13}C) = 15$ Hz), 69.5, 77.2, 77.3 ($J(^{195}Pt^{13}C) = 12$ Hz), 79.9 ($J(^{195}Pt^{13}) = 9.4$ Hz), 90.6, 144.4, 154.7, 160.2, 164.1, 165.3, 177.8.

This viscous material was stirred for 24 h with dilute hydrochloric acid (9 mL H_2O, 1 mL concentrated HCl) at room temperature and in the absence of air. A yellow solution and a gray platinum-containing solid were obtained. The precipitate was isolated by filtration and dried under vacuum. Anal. Found: C, 17.41; H, 3.83; N, 0.01. ^{1}H NMR ($CDCl_3$): δ −0.58 (m), −0.55 (s), −0.52 (s), −0.19 (s), −0.04 (s), 0.14 (s), 0.28 (s), 0.87 (s) 0.93 ($^2J(^{195}Pt^1H) = 78.31$ Hz), 1.07 (s), 1.13 (s), 1.16 (s), 1.19 (s), 1.22 (s), 1.24 (s), 1.29 (s), 1.38 (s).

The solution was adjusted to pH 9 using Na_2CO_3 and extracted three times with 10 mL of dichloromethane. The organic phases were combined, dried over 4 Å molecular sieve s, and examined via GC−MS (chemical ionization, M + 1 signals observed). MS (GC; t_R = 6.63−6.95 min): *m*/*z* 128, 112, 100, 84, 72. MS (GC: t_R = 8.82−9.02 min): *m*/*z* 130, 128, 114, 102, 86, 74, 72.

Using wavelengths above 515 nm for irradiation, cooling the solution to −20 °C, or adding nucleophilic pyridine as a possible ligand for free coordination sites formed at the metal did not result in higher selectivity of the photolysis. Photolysis at shorter wavelengths (λ > 400 nm, filter GG 400) led to the formation of a yellow-green solution, a black solid (Pt), and the evolution of gas (CH_4 as analyzed by GC). Removing the solvent from this solution yielded a yellow oily substance which gave essentially the same NMR spectra as the mixture obtained from irradiation at longer wavelengths.

Irradiating $PtMe_4$(*t*-Bu-DAB) in $CHCl_3$ or CH_2Cl_2 (λ > 400 nm) for 15 min resulted in the formation of a single species, which was crystallized from *n*-hexane in 70% yield and identified as $PtMe_3Cl$(*t*-Bu-DAB). Anal. Calcd (found) for $C_{13}H_{29}ClN_2Pt$ (443.94): C, 35.17 (34.76); H, 6.58 (6.31); N, 6.31 (6.15). ^{1}H NMR ($CDCl_3$): δ 0.62 (s, $^2J(^{195}Pt^1H) = 73.3$ Hz; $Pt-^{ax}CH_3$), 1.48(s, $^2J(^{195}Pt^1H) = 71.6$ Hz; $Pt-^{eq}CH_3$), 1.52 (s; $C(CH_3)_3$), 8.58 (s, $^3J(^{195}Pt^1H) = 20.8$ Hz; N*CH*).

For the photolysis of $PtMe_4$(*p*-Tol-DAB) acetone also proved to be the most suitable solvent. However, irradiation of this compound resulted in an even more complex mixture of products before and after hydrolysis; separation or identification of the products was thus not attempted.

Calculations. *Ab initio* Hartree−Fock (HF) and density-functional (DFT)/HF hybrid methods[17] were used in the calculation of $PtMe_n$(H-DAB) (*n* = 2,4). The GAUSSIAN 94 program package,[18a] Dunning's polarized valence double-ζ basis sets for the H, C, and N atoms,[18b] and a quasirelativistic energy-consistent pseudopotential with the corresponding optimized set of basis functions[19] for Pt were employed. The geometry optimization was always performed in C_{2v} constrained symmetry (DAB plane, *yz*; $C_{ax}-Pt-C_{ax}$ axis, *x*). Within the DFT/HF procedure, the three-parameter Becke−Lee−Yang−Parr (B3LYP) functional potential proved to be the most suitable.[7b]

Results and Discussion

Ground State and Calculation Results. Synthesis and Structure. The organoplatinum(II) and -(IV) compounds were obtained according to established methodology[4e,f,12−15] as thermally and oxidatively rather stable species; however, special care had to be taken regarding the light-sensitive Pt(IV) complexes of the α-diimine ligands. The complexes $PtMe_n$(TMEDA) are colorless, in contrast to all other species described here. The identity of the compounds was confirmed using elemental analysis and ^{1}H and ^{13}C NMR spectroscopy (Tables 1 and 2), the assignments being supported by spin−spin coupling patterns involving the ^{195}Pt isotope (33.3% natural abundance, $I = {}^1/_2$). The compound $PtMe_2$(*t*-Bu-DAB) could not be isolated due to insufficient conversion; $PtMes_2$(Cy-DAB) was not sufficiently soluble for NMR measurements but could be studied electrochemically and spectroscopically.

Dimesitylplatinum(II) complexes of aromatic α-diimines had been structurally characterized[4f,g] with

(17) Becke, A. D. *J. Chem. Phys.* **1993**, *98*, 5648.
(18) (a) Frisch, M. J.; Trucks, G. W.; Schlegel, H. B.; Gill, P. M. W.; Johnson, B. G.; Robb, M. A.; Cheeseman, J. R.; Keith, F. G. A.; Peterson, A.; Montgomery, J. A.; Raghavachari, K.; Al-Laham, M. A.; Zakrzewski, V. G.; Ortiz, J. V.; Foresman, J. B.; Cioslowski, J.; Stefanov, B. B.; Nanayakkara, A.; Challacombe, M.; Peng, C. Y.; Ayala, P. Y.; Chen, W.; Wong, M. W.; Andres, J. L.; Replogle, E. S.; Gomperts, R.; Martin, R. L.; Fox, D. J.; Binkley, J. S.; Defrees, D. J.; Baker, J.; Stewart, J. P.; Head-Gordon, M.; Gonzalez, C.; Pople, J. A. Gaussian 94, Revision B.3; Gaussian, Inc.: Pittsburgh, PA, 1995. (b) Dunning, T. H., Jr.; Hay, P. J. In *Modern Theoretical Chemistry*: *Methods of Electronic Structure Theory*; Schäfer, H. F., III, Ed.; Plenum: New York, 1977; Vol. 3.
(19) Andrae, D.; Häussermann, U.; Dolg, M.; Stoll, H.; Preuss, H. *Theor. Chim. Acta* **1990**, *77*, 123.

Table 2. ^{13}C-NMR Data of Platinum Complexes and Free Ligands in $CDCl_3$ at 25 °C[a]

compd	$Pt^{ax}CH_3$	$Pt^{eq}CH_3$	NCH	NC_1R^b	R
t-Bu-DAB			157.9	58.2	29.4
$PtMe_4$(*t*-Bu-DAB)	4.5 (444.2)	−4.5 (721.0)	155.8 (n.o.)	66.6 (16.2)	29.5
Cy-DAB			160.1	69.4	24.7, 25.5, 33.9
$PtMe_4$(Cy-DAB)	2.7 (442.4)	−7.2 (694.0)	155.4 (n.o.)	65.1 (18.4)	25.5, 25.6, 33.5
$PtMe_2$(Cy-DAB)		−15.1 (785.5)	158.3 (14.5)	65.0 (36.4)	25.6, 25.8, 33.8
p-Tol-DAB			159.1	147.6	21.1, 121.3, 130.0, 138.1
$PtMe_4$(*p*-Tol-DAB)	5.8 (448.0)	−4.2 (694.5)	157.2 (n.o.)	146.2 (16.3)	21.1, 122.0, 129.6, 138.7
$PtMe_2$(*p*-Tol-DAB)		−11.6 (799.0)	160.8 (n.o.)	147.3 (28.8)	21.1, 123.0, 129.5, 138.6
$PtMes_2$(*p*-Tol-DAB)			160.2	146.6	21.2, 123.1, 128.2, 138.6[c]
2,6-Xyl-DAB			163.4	149.8	18.2, 124.8, 126.4, 128.3
$PtMe_4$(2,6-Xyl-DAB)	14.6 (452.3)	−4.5 (690.7)	159.8 (n.o.)	146.8 (10.9)	19.7, 127.2, 128.8, 130.3
$PtMe_2$(2,6-Xyl-DAB)		−14.2 (793.5)	162.3 (9.5)	148.5 (n.o.)	17.5, 126.5, 127.7, 129.1
t-Bu-pyca[d]			155.6	57.0	28.9, 120.2, 123.6, 135.7, 148.4, 154.9
$PtMe_4$(*t*-Bu-Pyca)	3.66 (439.5)	−10.5 (720.7), −3.3 (729.5)	157.0 (n.o.)	65.9 (n.o.)	29.5, 125.9, 127.8 (14.9), 136.6, (6.2), 146.2 (15.8), 155.3
TMEDA			57.5[e]	45.6[f]	
$PtMe_4$(TMEDA)	12.5 (488.1)	−8.6 (746.5)	61.0[e]	48.3[f]	
$PtMe_2$(TMEDA)			−23.7 (826.9)	62.0[e]	49.0[f]

[a] Chemical shifts d in ppm, $J(195Pt^{13}C)$ coupling constants (in Hz) in parentheses, n.o. = not observed. [b] α-C-atom of substituent R. [c] Further signals at 27.2 (o-CH_3), 20.4 (p-CH_3), 125.7, 131.8, 138.7, 142.8 (phenyl C atoms). [d] From ref 9a. [e] NCH_2CH_2N. [f] $N(CH_3)_2$.

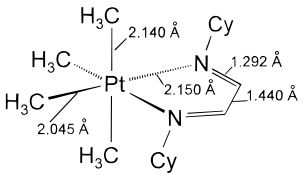

Figure 1. Essential bond lengths in $PtMe_4$(Cy-DAB) (Cy = cyclohexyl; from ref 4e).

Table 3. Comparison of Selected Experimental and Calculated Bond Lengths (Å)

		calcd[b]	
bond	exptl[a]	DFT/HF	HF
Pt−N	2.150	2.141	2.287
N−C (DAB)	1.292	1.304	1.256
C−C (DAB)	1.440	1.457	1.493
$Pt-C_{eq}$	2.045	2.069	2.032
$Pt-C_{ax}$	2.140	2.173	2.152

[a] For $PtMe_4$(CyN=CHCH=NCy), from ref 4e. [b] For $PtMe_4$-(HN=CHCH=NH).

approximately square-planar metal configuration and sterically protected axial positions; we therefore assume a similar situation for the compounds $PtMes_2$(R-DAB).

The tetramethylplatinum complex of CyN=CHCH=NCy had been structurally characterized before,[4e] showing (i) the chelate coordination of an essentially unperturbed 1,4-diaza-1,3-butadiene conjugated system and (ii) significantly longer Pt−C bonds to the axial methyl groups (2.140(8) Å) than to the equatorial CH_3 substituents (2.045(5) Å). (Figure 1).

Calculations. Quantum-chemical HF and hybrid DFT calculations as described in the previous section were applied to the simplified model compounds $PtMe_n$-(H-DAB) (n = 2, 4; H-DAB = HN=CHCH=NH). The problem of including a heavy 5d element was treated by means of a pseudopotential[19] which has proven successful in related previous cases.[7b]

The first aim of the calculations was to reproduce the structural results for $PtMe_4$(Cy-DAB).[4e] Table 3 summarizes essential results from experiment and calculations, the DFT approach giving clearly a better reproduction of the experimental structure, especially the Pt−N bond length.

For further discussion of calculated data we therefore use only the results from the DFT calculations, which

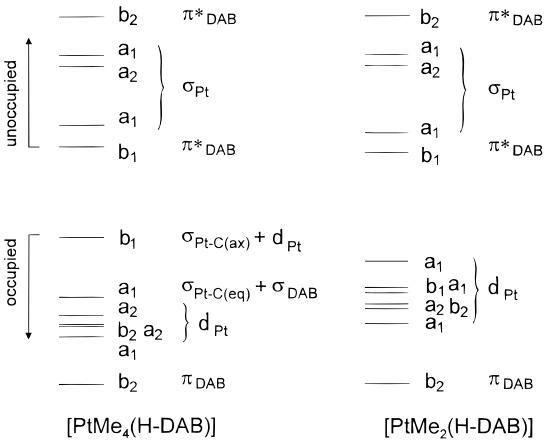

Figure 2. MO energy diagrams from DFT calculations (H-DAB = HN=CHCH=NH).

implicitly account for electron correlation effects. Defining the molecular axis of the complexes as z with the chelate ring lying in the yz plane, we arrive at molecular orbital sequences as depicted in Figure 2.

Whereas both the Pt(II) and Pt(IV) species have the π^*(R-DAB), supported by d_{xz}(Pt), as the lowest unoccupied MO (LUMO), the HOMO is primarily a metal centered d orbital for $PtMe_2$(R-DAB) but an antisymmetric $Pt-C_{ax}$ σ orbital combination (with some p_x(Pt) contributions) for $PtMe_4$(R-DAB). These results confirm a previous assignment[4e] and are in agreement with all further experimental evidence (see below). Figure 3 shows the frontier molecular orbitals for $PtMe_4$(R-DAB), clearly visualizing the assignments mentioned above.

For understanding the effects of reversible reduction,[4e,n] we also calculated the structural changes occurring on electron acquisition by $PtMe_n$(H-DAB) (Table 4). The effects are generally small but characteristic: DAB-centered reduction is expected[7b] to result in a lengthening of the C−N and a shortening of the C−C bonds. In agreement with results from EPR spectroscopy[4n] the calculated spin density on the metal is much lower in the Pt(IV) case (0.015) than for the Pt(II) complexes (0.149); consequently, the latter exhibit a distinctly higher g anisotropy[4n] than the former because of contributions from the metal with its high spin−orbit

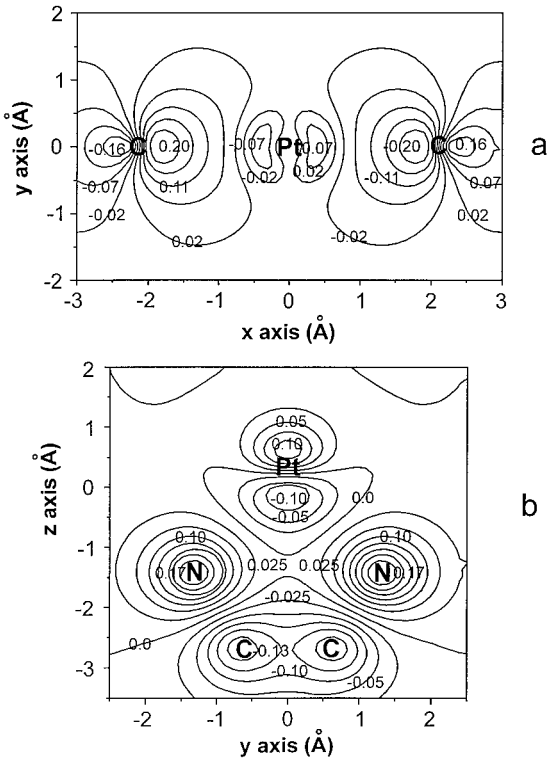

Figure 3. Contour diagrams for $PtMe_4$(H-DAB): (a) HOMO and (b) LUMO (0.5 Å above the PtNCCN plane).

Table 4. DFT/HF-Calculated Bond Lengths of Neutral Species and Radical Anions (Å)

	$[PtMe_4(HN{=}CHCH{=}NH)]^n$		$[PtMe_2(HN{=}CHCH{=}NH)]^n$	
bond	$n = 0$	$n = -1$	$n = 0$	$n = -1$
Pt−N	2.141	2.155	2.113	2.112
N−C (DAB)	1.304	1.345	1.305	1.350
C−C (DAB)	1.457	1.411	1.458	1.403
$Pt-C_{eq}$	2.069	2.070	2.050	2.068
$Pt-C_{ax}$	2.173	2.162		

coupling constant.[20] For the primarily spin-bearing chelate ligands in $[PtMe_n(R\text{-}DAB)]^{\bullet-}$ the calculated spin densities at the nitrogen centers vary just marginally (0.363 vs 0.330).

Oxidized and Reduced States. Electrochemistry. While all methylplatinum complexes are oxidized in an electrochemically fully irreversible fashion, the compounds $PtMes_2$(R-DAB) with the axially shielding mesityl groups exhibit still reversible oxidation waves in acetonitrile/0.1 M Bu_4NPF_6 (Figure 4).

As in related previous cases,[4f,g] we formulate these EPR-silent and only metastable ($t_{1/2}$ < 3 min) species $[PtMes_2(\alpha\text{-diimine})]^+$ as Pt(III) complexes, protected against rapid addition of nucleophiles (solvent) by blocking of the axial positions. This formulation is in agreement with the results from DFT calculations (Figure 2). Although oxidized at rather low potentials, the complexes $PtMe_n(\alpha$-diimine) display only irreversible electrochemical behavior (Table 4). The coordinatively unsaturated and axially unprotected $PtMe_2$ complexes probably react with nucleophilic constituents of the electrolyte on oxidation to the Pt(III) = $5d^7$ state.[4b] On the other hand, the $PtMe_4$ species are likely to undergo a $Pt-C_{ax}$ bond cleavage after removal of one binding electron from the corresponding σ orbital combination (Figure 2). Spectroelectrochemistry for the electrochemically irreversible oxidation of $PtMe_n$(R-DAB) in the UV−vis region (Figures S3 and S4; Supporting Information) yields isosbestic points which suggest relatively straightforward follow-up reactions.

(20) Weil, J. A.; Bolton, J. R.; Wertz, J. E. *Electron Paramagnetic Resonance*; Wiley: New York, 1994.

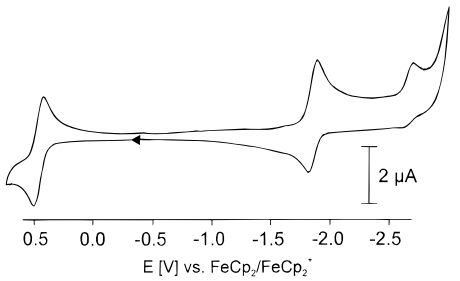

Figure 4. Cyclic voltammogram of $PtMes_2$(Cy-DAB) in THF/0.1 M Bu_4NPF_6 at 100 mV/s scan rate.

Table 5. Electrochemical Data of Platinum Complexes and Free Ligands[a]

compd	E_{pa}(ox)[b] or $E_{1/2}$(ox) (ΔE_{pp})[c]	$E_{1/2}$(redI) (ΔE_{pp})[c]	$E_{1/2}$(redII) (ΔE_{pp})[c]
t-Bu-DAB		−2.86[d]	
$PtMe_4$(*t*-Bu-DAB)	0.34[b]	−1.98 (76)	−2.28 (138)
$PtMe_4$(*t*-Bu-DAB)[e]	0.35[b]	−2.08 (98)	−2.37 (154)
$PtMe_2$(*t*-Bu-DAB)	*f*	−1.88 (95)	
Cy-DAB		−2.63[d]	
$PtMe_4$(Cy-DAB)	0.37[b]	−1.93 (81)	−2.11 (127)
$PtMe_2$(Cy-DAB)	0.47[b]	−1.84 (80)	−3.01 irr[d]
$PtMes_2$(Cy-DAB)	0.47 (84)[c]	−1.88 (95)	−3.09 irr[d]
p-Tol-DAB		−1.86[d,g]	
$PtMe_4$(*p*-Tol-DAB)	0.45[b]	−1.41 (58)	−2.12 (135)
$PtMe_2$(*p*-Tol-DAB)	0.65[b]	−1.36 (85)	−2.12 (175)
$PtMes_2$(*p*-Tol-DAB)	0.53 (83)[c]	−1.41 (95)	−2.17 (140)
2,6-Xyl-DAB		−2.10[d]	
$PtMe_4$(2,6-Xyl-DAB)	0.46[b]	−1.48 (68)	−2.10 (108)
$PtMe_2$(2,6-Xyl-DAB)	0.74[b]	−1.53 (80)	−2.55 (240)
t-Bu-Pyca		−2.74	
$PtMe_4$(*t*-Bu-Pyca)	0.24[b]	−2.06 (68)	
$PtMe_4$(*t*-Bu-Pyca)[e]	0.27[b]	−2.20 (105)	2.47[d]
$PtMe_4$(TMEDA)	0.35[b]		
$PtMe_2$(TMEDA)	0.19[b]		

[a] From cyclic voltammetry in acetonitrile/0.1 M Bu_4NPF_6; potentials in V vs $FeCp_2^{0/+}$, scan rate 100 mV s^{-1}. [b] Anodic peak potential for mostly irreversible oxidation. [c] Peak-to-peak separation $\Delta E_{pp} = E_{pc} - E_{pa}$ (mV). [d] Irreversible reduction, cathodic peak potential. [e] In THF/0.1 M Bu_4NPF_6. [f] Not available. [g] From ref 7a. [h] No reduction until −2.70 V.

More than the anodic peak potentials for organometal-centered oxidation, the reduction potentials reflect the substitution at the R-DAB ligands. The potentials increase with decreasing donor effect of R, viz., in the order *t*-Bu < Cy ≪ 2,6-Xyl < *p*-Tol. The complex with the unsymmetrical α-diimine *t*-Bu-Pyca exhibits rather negative reduction potentials. The second reduction processes at potentials below −2 V vs. $FeCp_2^{+/o}$ are not fully reversible. EPR studies have confirmed the occupation of the π^*(R-DAB) orbital on one-electron uptake but also revealed slow group transfer reactions of the reduced forms.[4n]

An unusual feature of the $PtMe_n$(R-DAB) species is that the cyclic voltammograms for $n = 2$ and $n = 4$

Table 6. Long-Wavelength Absorption Maxima λ_{max} (nm) of Platinum Complexes

compd	solvent	λ_{max} (ϵ)[a]
$PtMe_4$(*t*-Bu-DAB)	CH_3CN	307 sh; 471
$PtMe_4$(*t*-Bu-DAB)	toluene	322 (1.75); 520 (9.5)
$PtMe_2$(*t*-Bu-DAB)	Et_2O	385 sh, 400; 492 sh; 535 sh, 575
$PtMe_4$(Cy-DAB)	CH_3CN	311; 485
$PtMe_4$(Cy-DAB)	toluene	326 (1.85); 506 sh, 532 (1.05)
$PtMe_2$(Cy-DAB)	CH_3CN	376; 504 sh; 531
$PtMe_2$(Cy-DAB)	toluene	391 sh, 400 (4.9); 498 sh, 536 (2.1),[a] 578 (3.4); 638 (0.07)[b]
$PtMes_2$(Cy-DAB)	CH_2Cl_2	355; 441; 483 sh, 532, 590 sh
$PtMes_2$(Cy-DAB)	toluene	357 sh; 440 sh, 463; 505, 540, 605 sh
$PtMe_4$(*p*-Tol-DAB)	CH_3CN	344, 380 sh; 462 sh; 563
$PtMe_4$(*p*-Tol-DAB)	toluene	355 (8.4); 484 sh; 617 (1.2)
$PtMe_2$(*p*-Tol-DAB)	CH_3CN	321 sh, 380; 508 sh; 559 sh, 598
$PtMe_2$(*p*-Tol-DAB)	toluene	470 sh, 550 sh (1.3); 604 sh, 656 (3.3)
$PtMes_2$(*p*-Tol-DAB)	CH_3CN	374; 598
$PtMes_2$(*p*-Tol-DAB)	toluene	385; 556 sh, 632
$PtMe_4$(2,6-Xyl-DAB)	CH_3CN	340, 373 sh; 550
$PtMe_4$(2,6-Xyl-DAB)	toluene	354, 393 sh; 483 sh; 605
$PtMe_2$(2,6-Xyl-DAB)	CH_3CN	390; 547 sh, 586
$PtMe_2$(2,6-Xyl-DAB)	toluene	394; 537 sh, 596, 634
$PtMe_4$(*t*-Bu-Pyca)	CH_3CN	304; 347 sh; 449
$PtMe_4$(*t*-Bu-Pyca)	toluene	318; 363 sh; 493

[a] Molar extinction coefficients ϵ (10^3 M^{-1} cm^{-1}). [b] ^{3}MLCT absorption; from band deconvolution.

species look very much alike.[4e] Reversible R-DAB-centered reduction and irreversible oxidation, either of the metal (Pt^{II} compounds) or of the Pt−C_{ax} σ bonds (Pt^{IV} complexes), occur at very similar potentials (Table 5). Obviously, the binding of two additional methyl carbanions compensates almost exactly for the effect of the higher metal oxidation state.

Excited States. Absorption Spectra and Reorganization Energy. Except for the TMEDA complexes which lack a low-lying π*-orbital, all other platinum compounds are intensely colored due to charge-transfer absorptions in the visible region (Table 6).

According to the calculated (Figure 2) and previously assumed[4e] electronic situation, the PtR'_2(α-diimine) compounds should exhibit long-wavelength MLCT transitions from high-lying occupied d orbitals to π* orbitals of the α-diimines; the tetraalkylplatinum fragments, on the other hand, have stabilized metal d orbitals ($5d^6$ situation) but high lying platinum-methyl σ bonds of which the highest lying antisymmetric combination[21,22] of the two σ(Pt−C_{ax}) orbitals is well suited for engaging in ligand(Me)-to-ligand(R-DAB) charge transfer ($L_\sigma L_{\pi^*}$-CT).

The simplicity of the complexes studied here allowed us to observe and interpret band structuring due to vibrational contributions. (Compounds with aromatic α-diimines exhibit far more extensive overlap of CT bands.[4]) The $PtMe_2$ complexes with their small number of degrees of freedom invariably exhibit structured long-wavelength bands; Figure 5 shows one such feature with applied deconvolution. There is a weak broad band at the low-energy side which we assign to a ^{3}MLCT

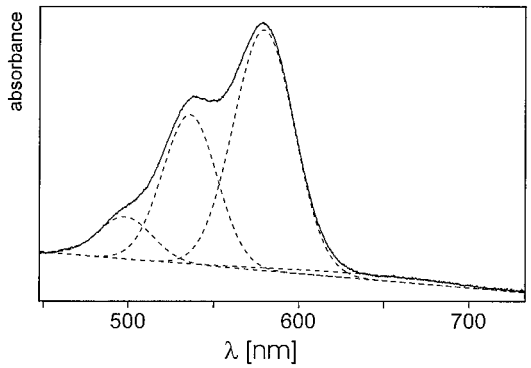

Figure 5. Deconvolution of the long-wavelength MLCT absorption band of $PtMe_2$(Cy-DAB) in toluene.

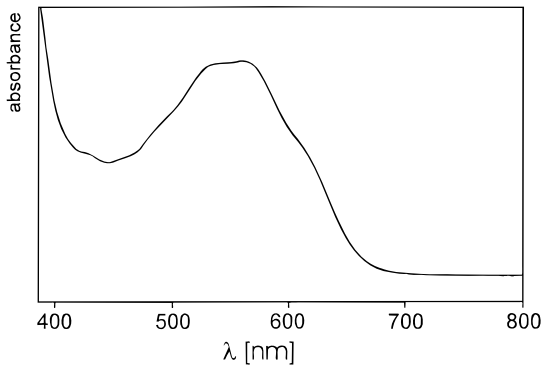

Figure 6. Long-wavelength LLCT absorption band of $PtMe_4$(*t*-Bu-DAB) in CS_2 solution.

absorption, detectable here because of the high spin−orbit coupling constant of Pt,[20] and there are at least three discernible components of the singlet absorption system spaced at about 1400 cm^{-1}—a typical vibration energy for α-diimines.[23]

The $PtMe_4$ complexes have more degrees of freedom and do not usually exhibit LLCT band structuring except in extremely nonpolar solvents such as CS_2 (Figure 6).

Figure 6 shows that the $PtMe_4$ complexes also differ from the $PtMe_2$ species by not having the long-wavelength component as the most intense feature. The spectroscopic result is a poorer resolution and a close to Gaussian band shape. These conspicuous differences suggest a higher amount of geometrical reorganization on LLCT excitation of the Pt(IV) species through changes in the Pt-C σ bonds. In contrast, the overall amount of reorganization is quite small for the Pt(II) species, as evident from the following estimation.[4f,24,25] For $PtMes_2$(*p*-Tol-DAB), the energy at the absorption maximum is 598 nm = 2.07 eV in acetonitrile (cf. Table S7; Supporting Information). In the same solvent, the difference between oxidation and reduction half-wave potentials is 0.53 V − (−1.41 V) = 1.94 V (Table 5). Accordingly, the approximation $\chi = E_{op}$ [eV] − (E_{ox} − E_{red}) [V] for Franck−Condon contributions from intra-

(21) Kaupp, M.; Stoll, H.; Preuss, H.; Kaim, W.; Stahl, T.; van Koten, G.; Wissing, E.; Smeets, W. J. J.; Spek, A. K. *J. Am. Chem. Soc.* **1991**, *113*, 5606.

(22) (a) Kaim, W. *Top. Curr. Chem.* **1994**, *169*, 231. (b) Hasenzahl, S.; Kaim, W.; Stahl, T. *Inorg. Chim. Acta* **1994**, *225*, 23.

(23) Nieuwenhuis, H. A.; Stufkens, D. J.; McNicholl, R.-A.; Al-Obaidi, A. H. R.; Coates, C. G.; Bell, S. E. J.; McGarvey, J. J.; Westwell, J.; George, M. W.; Turner, J. M. *J. Am. Chem. Soc.* **1995**, *117*, 5579.

(24) (a) Kober, E. M.; Goldsby, K. A.; Narayana, D. N. S.; Meyer, T. J. *J. Am. Chem. Soc.* **1983**, *105*, 4303. (b) Curtis, J. C.; Sullivan, B. P.; Meyer, T. J. *Inorg. Chem.* **1983**, *22*, 224.

(25) (a) Dodsworth, E. S.; Lever, A. B. P. *Chem. Phys. Lett.* **1985**, *119*, 61. (b) Dodsworth, E. S.; Lever, A. B. P. *Chem. Phys. Lett.* **1986**, *124*, 152.

Table 7. Correlation of Charge-Transfer Transition Wavenumbers ν_{CT} of Platinum Complexes with the Solvent Parameter E^*_{MLCT}[a] ($\nu_{CT} = A + BE^*_{MLCT}$)

	MLCT			LLCT		
complex	A (cm^{-1})	B (cm^{-1})	r[b]	A (cm^{-1})	B (cm^{-1})	r[b]
$PtMe_4$(*t*-Bu-DAB)	30 540	2 060	0.968	18 400	2 960	0.996
$PtMe_4$(Cy-DAB)	30 020	2 240	0.972	18 230	2 610	0.983
$PtMe_4$(*p*-Tol-DAB)				15 530	2 350	0.997
$PtMe_4$(bpy)[c]				20 210	2 640	0.993
	MLCT II			MLCT I		
complex	A (cm^{-1})	B (cm^{-1})	r[b]	A (cm^{-1})	B (cm^{-1})	r[b]
$PtMe_2$(Cy-DAB)	24 370	2 400	0.967	16 520	2 210	0.988
$PtMe_2$(*p*-Tol-DAB)				14 730	2 070	0.993
$PtMe_2$(bpy)[d]				18 610	3 340	0.995
$PtMes_2$(Cy-DAB)	20 490	3 350	0.959	18 040	1 390	0.911
$PtMes_2$(*p*-Tol-DAB)	25 590	1 140	0.984	15 470	1 340	0.979

[a] From ref 27. [b] r = correlation coefficient. [c] Calculated from data given in ref 32. [d] Calculated from data given in ref 35.

and intermolecular reorganization[24,25] yields $\chi = 0.14$ (e)V, which is a rather small number when compared e.g. to corresponding values of about 0.25 (e)V for [Ru(α-diimine)$_3$]$^{2+}$ complex ions.[25]

Solvatochromism. Charge-transfer transitions are usually quite solvent dependent,[26−28] unless strong interactions between the components cause significant orbital mixing. Typically, the CT transition dipole moment in coordination compounds lies opposite to the molecular dipole which reduces the polarity in the excited state and causes long-wavelength shifts in less polar solvents ("negative solvatochromism"). Like several other platinum complexes of α-diimines and related acceptor ligands,[3,4] the compounds described here are indeed solvatochromic in the described sense. The data for the long-wavelength absorption maxima are summarized for some selected examples in Tables S1−S7 (Supporting Information); attempts to correlate these values with established solvent parameters showed a very satisfactory correlation in all instances with the E^*_{MLCT} values which were derived by Manuta and Lees for the MLCT transition of (bpy)M(CO)$_4$ compounds (bpy = 2,2′-bipyridine; M = W).[27] The results of these correlations are listed in Table 7.

These correlations confirm that the compounds with aromatic substituents R in R-DAB have generally lower CT transition energies (low A values) due to a strongly stabilized π^* orbital. The sensitivity of the complexes toward solvation as expressed by the gradient B in the correlation equation $\nu_{max} = A + B \times E^*_{MLCT}$ is generally high for the LLCT transitions of the $PtMe_4$(α-diimine) compounds, indicating very little orbital mixing. In the PtR_2(α-diimine) complex series there is a larger amount of variation for the long-wavelength MLCT bands. The bpy complex shows strong solvent dependence, followed by $PtMe_2$(R-DAB) species with less pronounced effects and by the relatively slightly solvent-sensitive compounds $PtMes_2$(R-DAB). Part of this variation may lie in the open structure of the $PtMe_2$ systems, which may at least to some extent engage in specific solute-solvent interactions involving π systems.[29] The smaller solvatochromism of the shielded PtR'_2 system probably reflects a higher degree of orbital mixing as deduced also from EPR spectroscopy of the reduced forms.[4n]

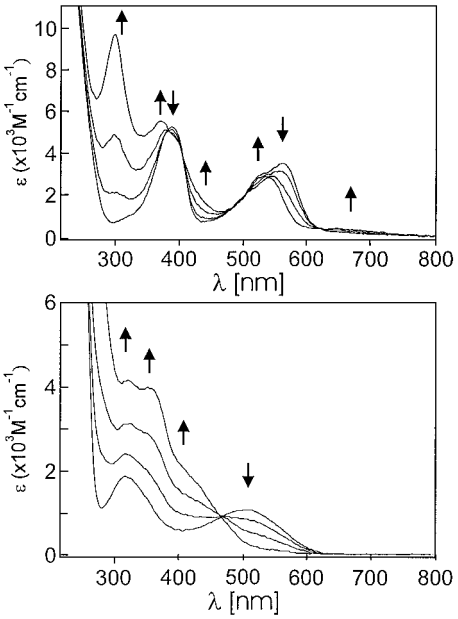

Figure 7. Spectroelectrochemical response on reduction of $PtMe_n$(Cy-DAB) in THF/0.1 M Bu_4NPF_6: (top) $n = 2$; (bottom) $n = 4$.

Spectroelectrochemistry. Using an OTTLE cell,[10] we could study both the reversible reduction and the electrochemically irreversible oxidation of the organoplatinum compounds. Figures 7 and S1−S4 show examples for corresponding spectral changes; Table 8 summarizes the data.

For the diorganoplatinum(II) compounds the long-wavelength CT bands appear slightly shifted and there are additional weak features emerging between 700 and 800 nm. In case of the tetramethylplatinum(IV) complexes the LLCT band is shifted to higher energies; for R = *p*-Tol there are still long-wavelength bands remaining, as is also observed for the noncoordinated ligand anion (Table 8); intense bands appear on reduction around 400 nm in both instances. At this point, we are unable to assign the emerging bands with sufficient

(26) (a) Lever, A. B. P. *Inorganic Electronic Spectroscopy*, 2nd ed.; Elsevier: Amsterdam, 1984; p 776. (b) Reichardt, C. *Solvents and Solvent Effects in Organic Chemistry*, 2nd ed.; VCH: Weinheim, Germany, 1988.

(27) Manuta, D. M.; Lees, A. J. *Inorg. Chem.* **1983**, *22*, 3828.

(28) Kaim, W.; Kohlmann, S.; Ernst, S.; Olbrich-Deussner, B.; Bessenbacher, C.; Schulz, A. *J. Organomet. Chem.* **1986**, *302*, 211.

(29) Kaim, W.; Olbrich-Deussner, B.; Roth, T. *Organometallics* **1991**, *10*, 410.

Table 8. Long-Wavelength Absorption Maxima of Anion Radical Compounds[a]

compd	λ_{max} (ϵ)[b]
[$PtMe_4$(*t*-Bu-DAB)]$^{\bullet-}$	350 (7.1), 394 sh, 449 sh
[Cy-DAB]$^{\bullet-}$ [c]	320, 360, 400 sh, 495 sh
[$PtMe_4$(Cy-DAB)]$^{\bullet-}$	320 (4.3), 354 (4.1), 413 sh
[$PtMe_2$(Cy-DAB)]$^{\bullet-}$	298 (9.8), 371 (5.4), 400 sh, 540 (2.8), 650 (0.4)
[*p*-Tol-DAB]$^{\bullet-}$ [c]	299, 460, 551 sh, 634, 677 sh, 942
[$PtMe_4$(*p*-Tol-DAB)]$^{\bullet-}$	345 (5.7), 407 sh, 460 (17.3), 513 sh, 590 sh
[$PtMe_2$(*p*-Tol-DAB)]$^{\bullet-}$	399 (16.5), 435 (14.0), 483 sh, 642 (3.0), 780 (1.55)
[$PtMes_2$(*p*-Tol-DAB)]$^{\bullet-}$	374 sh, 406, 496 sh, 583, 740
[$PtMe_4$(2,6-Xyl-DAB)]$^{\bullet-}$	370 sh, 433, 492 sh
[$PtMe_2$(2,6-Xyl-DAB)]$^{\bullet-}$	297, 379 sh, 423, 463 sh, 607, 671 sh, 750

[a] Generated by cathodic reduction of neutral compounds in 0.1 M Bu_4NPF_6/THF solution (OTTLE spectroelectrochemistry). [b] Absorption maxima in nm, molar extinction coefficients ϵ (in 10^3 M^{-1} cm^{-1}) in parentheses. [c] Generated chemically by reduction with potassium in THF.

confidence; excited-state calculations of open-shell systems involving such heavy elements are currently beyond our computational capability.

Interestingly, the electrochemically irreversible oxidation reactions of both the $PtMe_2$(R-DAB) and $PtMe_4$(R-DAB) compounds proceed spectroelectrochemically via spectra series with isosbestic points (Figures S3 and S4), which suggests rather straightforward reactions; the CT bands disappear in the course of this reaction. Product analyses of these reactions are currently under investigation.

Reactions with Light: Emission and Photoreactivity. A large number of platinum(II) complexes have already been studied with respect to photoemission from MLCT or other excited states.[3] Effects of the ligation, of the structure, and of the environment were intensely researched. It is not surprising, therefore, that the $PtMe_2$(R-DAB) compounds described here are also photoemissive. In the following we present the results of a preliminary such study, dealing with two representative examples (Table 9, Figures 8 and S5).

As Figure 8 demonstrates, the irradiation into the low-energy band (MLCT I) of $PtMe_2$(Cy-DAB) at ambient temperature in toluene solution produces a weak emission at longer wavelengths, the main absorption and emission maxima differing by 1430 cm^{-1}. Irradiation into the high-energy band (MLCT II) produces a stronger response and a different emission spectrum (Figure S5, Table 9) with a maximum at higher energies; the difference between the absorption and emission maxima is larger here at 3260 cm^{-1}. Obviously, there are at least two excited states available for luminescence which may occur from ^{3}MLCT excited states (at lower energy) and from intraligand excited states. There is little difference between the complexes with Cy-DAB and *p*-Tol-DAB ligands (Table 9). Clearly, the photophysical response of these species warrants further investigation with respect to solvent and temperature variation, quantum yield determination, and lifetime measurements. Nevertheless, it is apparent that the Pt(II) compounds are photostable and emissive.

In stark contrast to this response of PtR'_2(R-DAB) compounds toward irradiation, the $PtMe_4$(R-DAB) species show chemical reactivity on exposure to even long-wavelength visible light. In a recent EPR study[4n] we have proposed a photoinduced Pt−C_{ax} bond homolysis caused by the $L_\sigma L_{\pi^*}$CT process, based on related interpretations in e.g. zinc, aluminum, gallium, cobalt, manganese, rhenium, or ruthenium organometallic chemistry.[21,22,30] The platinum-containing fragment of that homolysis could be spin-trapped using 2-methyl-2-nitrosopropane.[4n]

Following these EPR results and the successful use of related organozinc compounds in organic synthesis, for example, of β-lactams,[31] we have studied the preparative photochemistry of $PtMe_4$(R-DAB) (R = *t*-Bu, *p*-Tol). In chlorinated methane solvents (CH_2Cl_2, $CHCl_3$) we observed the familiar[32] reaction to $PtMe_3Cl$(α-diimine). In acetone, irradiation at higher energies (400 < λ < 500 nm) caused decomposition for R = *t*-Bu with formation of platinum metal and some methane, whereas the filter-controlled irradiation into the LLCT band (λ > 475 nm) resulted in rapid bleaching, even when only the long-wavelength foot of the band was concerned. Isosbestic points were not observed by UV−vis absorption spectroscopy, indicating a more complicated reaction mechanism. Workup of the resulting colorless solutions, including eventual hydrolysis, led always to a mixture of products. In case of the *t*-Bu-DAB complex, we could observe by NMR several oligo(methylplatinum)-containing intermediate complexes and —after hydrolysis and removal of an R-DAB-free precipitate—by GC−MS two metal-free but chemically sensitive amino aldehyde products (Scheme 1) with *m*/*z* 130 (one of two possible isomers) and 128 (M + 1 peaks following chemical ionization).

These products are well-known from heat- or light-induced group transfer reactions involving ZnR_2(R-DAB) complex intermediates.[21,31,33] However, under the conditions employed here they are formed in a nonselective fashion, which disfavors their use in organic synthesis. Nevertheless, following previous concepts and interpretations of the photoreactivity of species MR'_n(R-DAB)[21,22] we assume a mechanistic pathway (Scheme 1) involving the homolysis of one metal−carbon (alkyl) bond, prompted by intramolecular electron transfer from the antisymmetric M−C_{ax} σ* combination to the π* level of R-DAB. (Remarkably, when one axial methyl group is replaced by a halide ligand, the system becomes photostable.) The loss of one binding σ electron is eventually responsible for the bond cleavage which may then proceed (i) via recombination to the starting material,

(30) (a) Daikh, B. E.; Finke, R. G.; *J. Am. Chem. Soc.* **1991**, *113*, 4160. (b) Rossehaar, B. D.; Kleverlaan, C. J.; Stufkens, D. J.; Oskam, A. *J. Chem. Soc., Chem. Commun.* **1994**, 63. (c) Niewenhuis, H. A.; van de Ven, M. C. E.; Stufkens, D. J.; Oskam, A.; Goubitz, K. *Organometallics* **1995**, *14*, 780. (d) Finger, K.; Daniel, C. *J. Chem. Soc., Chem. Commun.* **1995**, 1427. (e) Nieuwenhuis, H. A.; van de Ven, M. C. E.; Stufkens, D. J.; Oskam, A.; Goubitz, K. *Organometallics* **1995**, *14*, 780. (f) Rossenaar, B. D.; Kleverlaan, C. J.; van de Ven, M. C. E.; Stufkens, D. J.; Vlcek, A., Jr. *Chem. Eur. J.* **1996**, *2*, 228.

(31) (a) Klerks, J. M.; Jastrzebski, J. T. B. H.; van Koten, G.; Vrieze, K. *J. Organomet. Chem.* **1982**, *224*, 107. (b) van Koten, G. In *Organometallics in Organic Synthesis*; de Meijere, A., tom Dieck, H., Eds.; Springer-Verlag: Berlin, 1987, p 277. (c) Wissing, E.; Rijnberg, E.; van der Schaaf, P. A.; Garp, K. V.; Boersma, J.; van Koten, G. *Organometallics* **1994**, *13*, 2609. (d) Rijnberg, E.; Boersma, J.; Jastrzebski, J. T. B. H.; Lakin, M. T.; Spek, A. L.; van Koten, G. *Organometallics* **1997**, *16*, 3158.

(32) Hux, J. E.; Puddephatt, R. J. *J. Organomet. Chem.* **1992**, *432*, 251.

(33) van Koten, G.; Jastrzebski, J. T. B. H.; Vrieze, K. *J. Organomet. Chem.* **1983**, *250*, 46.

Scheme 1. Proposed Reaction Mechanism of Photoinduced Group Migration in the Compounds $PtMe_4$(R-DAB).

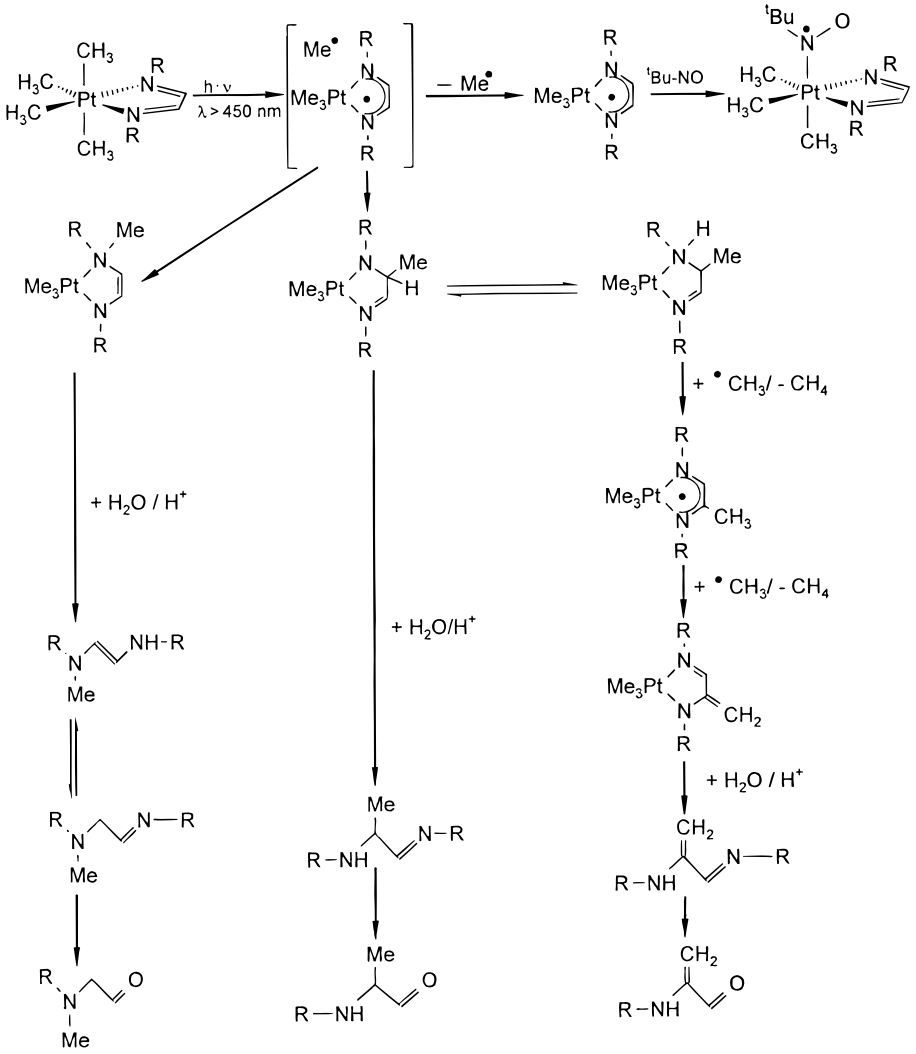

Table 9. Long-Wavelength Emission Maxima of Platinum(II) Complexes

	emission			corresponding absorption		
compd	λ_{em} (nm)	ν_{em} (cm^{-1})	λ_{ex} (nm)[a]	λ_{abs} (nm)	ν_{abs} (cm^{-1})	Δ (cm^{-1})[b]
$PtMe_2$(Cy-DAB)	460	21 740	400	400	25 000	3 260
$PtMe_2$(Cy-DAB)	630	15 870	578	578	17 300	1 430
$PtMe_2$(*p*-Tol-DAB)	460	21 740	400	398[c]	25 130	3 390

[a] Wavelength of excitation. [b] Δ defined as $\nu_{abs} - \nu_{em}$. [c] Intraligand transition.

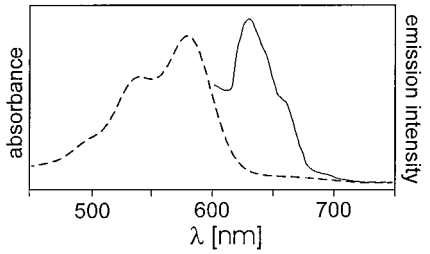

Figure 8. Absorption (- - -) and emission spectra (—) of $PtMe_2$(Cy-DAB) in toluene at ambient temperature (excitation at 578 nm).

(ii) via dissociation to free radicals and their follow-up products,[4n] or (iii) via the "cage reaction" to metal-to-ligand group transfer (N, C-alkylation) and subsequent rearrangement and equilibration, H abstraction and eventual hydrolysis. There is evidence for double alkylation from the NMR comparison with complexes of fully saturated TMEDA (Tables 1 and 2) and for the formation of methylene functions. Following a previous interpretation[31c] we attribute this latter reaction to the 2-fold hydrogen abstraction by alkyl radicals (Scheme 1). Activation of the axial metal−carbon bonds is not only evident from experimental (Figure 1) and calculated (Table 2) bond lengths but also from a very intense infrared band at 470−480 cm^{-1} for the complexes $PtMe_4$-(R-DAB), which we assign to the asymmetric stretching motion of $C_{ax}-Pt-C_{ax}$.

In summary, the present study delineates how two related classes of simple organometallic compounds with—at first sight—similar spectroscopic and electrochemical features differ with regard to their electronic structure (experiment, theory) and reactivity. In addition to the differences observed on organometal-centered

oxidation and R-DAB ligand-centered reduction (no evidence for "Pt(I)" states[4a,34]) there is a striking dichotomy concerning the low-lying excited states and the response to irradiation with light. Whereas the complexes PtR'_2(R-DAB) have an emissive MLCT lowest energy excited state, the corresponding PtR'_4(R-DAB) species are highly photoreactive from an $L_\sigma L_{\pi^*}$CT excited state.

(34) Fanizzi, F. P.; Natile, G.; Lanfranchi, M.; Tiripicchio, A.; Laschi, F.; Zanello, P. *Inorg. Chem.* **1996**, *35*, 3173.
(35) Chaudhury, N.; Puddephatt, R. J. *J. Organomet. Chem.* **1975**, *84*, 105.

Acknowledgment. We thank the Volkswagenstiftung, Deutsche Forschungsgemeinschaft, and Fonds der Chemischen Industrie for financial support.

Supporting Information Available: Tables S1−S7, giving absorption spectral data of complexes PtR'_n(R-DAB) in various solvents, Figures S1−S4, giving absorption spectra (spectroelectrochemistry), and Figure S5, giving the emission spectrum (15 pages). Ordering information is given on any current masthead page.

OM970736D